Water-Soluble Full-Length Single-Wall Carbon Nanotube Polyelectrolytes: Preparation and Characterization

Hanna Paloniemi,*,†,‡ Timo Ääritalo,† Taina Laiho,‡,§ Hanna Liuke,† Natalia Kocharova,† Keijo Haapakka,† Fabio Terzi,# Renato Seeber,# and Jukka Lukkari*,†

Department of Chemistry, University of Turku, 20014 Turku, Finland, Graduate School of Materials Research, Turku, Finland, Department of Physics, University of Turku, 20014 Turku, Finland, and Department of Chemistry, Universitá di Modena e Reggio Emilia, Via G. Campi 183, 41100 Modena, Italy

Received: December 14, 2004

HiPco single-wall carbon nanotubes (SWNTs) have been noncovalently modified with ionic pyrene and naphthalene derivatives to prepare water-soluble SWNT polyelectrolytes (SWNT-PEs), which are analogous to polyanions and polycations. The modified nanotubes have been characterized with UV−vis−NIR, fluorescence, Raman and X-ray photoelectron spectroscopy (XPS), and transmission electron microscopy (TEM). The nanotube−adsorbate interactions consist of $\pi-\pi$ stacking interactions between the aromatic core of the adsorbate and the nanotube surface and specific contributions because of the substituents. The interaction between nanotubes and adsorbates also involves charge transfer from adsorbates to SWNTs, and with naphthalene sulfonates the role of a free amino group was important. The ionic surface charge density of the modified SWNTs is constant and probably controlled by electrostatic repulsion between like charges. The linear ionic charge density of the modified SWNTs is similar to that of common highly charged polyelectrolytes.

Introduction

Single-wall carbon nanotubes (SWNTs) are one-dimensional (1D) forms of carbon, which can be regarded as cylinders formed upon rolling up a graphene sheet along a chiral (or roll-up) vector. In addition to being aesthetically pleasing structures, they possess unique electronic, mechanical, and thermal properties, which suggest a wide range of applications for these materials.[1] They can be prepared in several ways but the fundamental limitation to the use of the pristine material is its intractability as the very high attraction between individual nanotubes leads to the formation of large bundles and ropes. The poor solubility of pristine nanotubes in common solvents hampers their basic research at the molecular level, the development of solution-phase separation methods, and the controlled deposition and self-assembly of SWNTs.

Chemical modification of the side walls, defect sites, and open ends have been used to impart solubility to carbon nanotubes.[2] Especially, the solubilization in aqueous media is essential in improving the biocompatibility of the nanotubes and enabling their environmental-friendly characterization, separation, and self-assembly. Oxidatively shortened single-wall nanotubes are inherently soluble in water owing to ionic defects at the side walls and tube ends. The tube ends and side walls can also be functionalized by water-solubilizing agents.[3] The use of cut nanotubes, however, sacrifices one essential property of the as-produced carbon nanotubes: their extremely high aspect ratio. In addition, covalent modification of the tube side walls impairs the electronic structure of the tubes. Although the original electronic structure can be regained by thermal treatment, this can be detrimental to applications involving delicate materials, for example, biological macromolecules. Therefore, noncovalent side wall functionalization techniques are desirable, as they leave the electronic structure of the tubes intact. One strategy to exfoliate the bundles and to stabilize isolated SWNTs in an aqueous solution is to overcome the hydrophobic interactions between the tubes by repulsion forces. Accordingly, surfactants[4,5] and water-soluble polymers[6] facilitate the dissolution of SWNTs in water. Another strategy is to anchor ionic charges on the SWNT surface via suitable linker groups. Several aromatic molecules adsorb on graphite, and porphyrins,[7] pyrene,[8] and anthracene[9] derivatives have been reported to interact with nanotube side walls by $\pi-\pi$ stacking. Water-solubility and biocompatibility have been achieved with nanotubes containing adsorbed pyrene or porphyrin derivatives.[7b,8a−c]

The adsorption of the aromatic molecules is generally assumed to take place in a coplanar geometry with $\pi-\pi$ stacking in analogy with the graphene surface.[10] The strength of the $\pi-\pi$ interactions is expected to scale with the size of the aromatic moiety but, owing to the curvature of the nanotube surface, the shape of the ring system may also influence the affinity. In a polar medium, the major contributions to the $\pi-\pi$ stacking result from the electrostatic interactions and hydrophobic effects.[11] With molecules containing heteroatoms, the atom$-\pi$ electron interactions are important, which suggests that the substituents may have a role in controlling the $\pi-\pi$ interactions. Charge-transfer (CT) interactions have also been suggested to be involved in the noncovalent side wall modification of SWNTs with aromatic molecules but their role has not been thoroughly examined. Adsorbates containing a single aromatic ring have not been reported, but charge-transfer interactions have been suggested between benzene derivatives and SWNTs,[12] on the basis of electronic transport measurements, and also between nanotubes and amines[13,14] or ammonia.[15] Murray et al. found a correlation between the acceptor properties of anthracene

* To whom correspondence should be addressed. E-mails: jukka.lukkari@utu.fi; hanna.paloniemi@utu.fi.
† Department of Chemistry, University of Turku.
‡ Graduate School of Materials Research.
§ Department of Physics, University of Turku.
# Universitá di Modena e Reggio Emilia.

10.1021/jp0443097 CCC: $30.25
Published on Web 04/05/2005

CHART 1: Ionic Aromatic Molecules Used in This Work

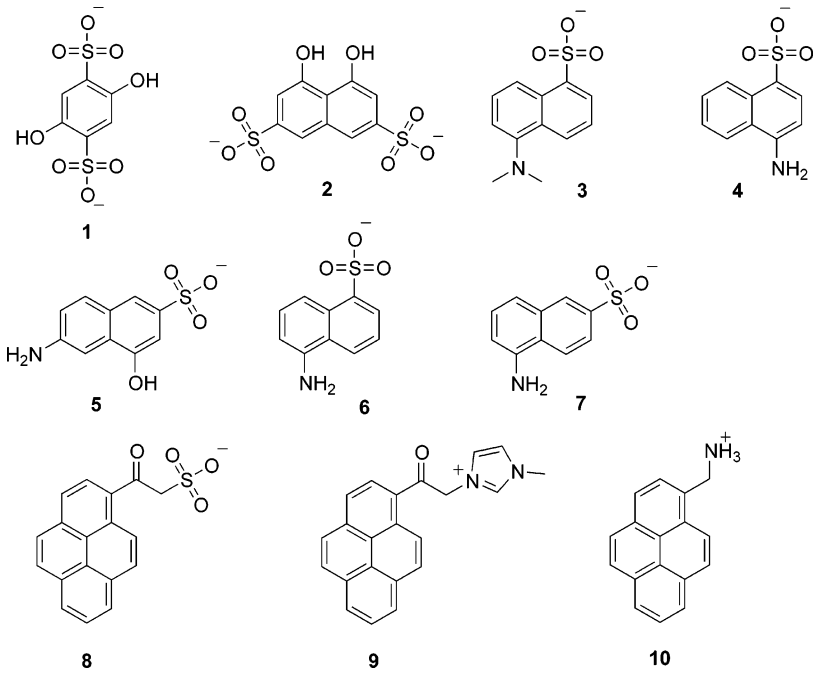

derivatives and the extent of adsorption on the SWNT surface.[9] The interaction between streptavidin and nanotubes has also been suggested to involve charge transfer from the amino groups in the protein.[16] However, an optical CT band reported for a suggested SWNT−aniline complex has recently been shown to result from aniline degradation products.[17]

In this paper, we study the capacity of various ionic aromatic molecules (Chart 1) to adsorb on carbon nanotube side walls and to solubilize SWNTs in aqueous medium. A comprehensive physicochemical characterization of the noncovalent modification of carbon nanotubes with aromatic compounds has not been reported. The smallest aromatic system described for the noncovalent modification has been anthracene but the interactions between the anthracene derivatives and SWNTs are relatively weak as these adsorbates can easily be desorbed from the surface.[9] Here, we show that, in addition to pyrenes, efficient modification and water-solubilization of SWNTs is possible by using naphthalenes with an even smaller ring system. Especially, we study the influence of naphthalene and pyrene substitution and the possible role of the substituents on the aromatic ring in the interactions with the nanotube surface. We explore the role of the charge transfer between SWNTs and the compounds in Chart 1 and seek to find correlations between the adsorbate structure and the properties of the noncovalently modified carbon nanotubes. In addition, water-soluble nanotubes with tethered ionic groups have a strong resemblance to polyelectrolytes or polyelectrolyte gels, a fact that has not been emphasized. Here, we coin the term single-wall carbon nanotube polyelectrolytes (SWNT-PEs) to describe these materials and discuss their polyelectrolyte-type properties.

Experimental Section

Materials. 4-Amino-1-naphthalenesulfonic acid (**4**, Aldrich, 97%), 6-amino-4-hydroxynaphthalene-2-sulfonic acid (**5**, Aldrich, 95%), 5-aminonaphthalene-1-sulfonic acid (**6**, Fluka, 98%), and 5-aminonaphthalene-2-sulfonic acid (**7**, Aldrich, 97%) were recrystallized from boiling water. 2,5-Dihydroxy-1,4-benzenedisulfonic acid, di-K-salt (**1**, Aldrich, 98%), 1,8-dihydroxy-3,6-naphthalenedisulfonic acid, di-Na-salt (**2**, Merck, pro analysi), 5-(dimethylamino)-1-naphthalenesulfonic acid (**3**, EGA-Chemie, 99+ %), 1-pyrenemethylamine, hydrochloride (**10**, 95%, Aldrich), and all the other chemicals were used as received. Water distilled twice in a quartz-distillation apparatus was used in all experiments.

Syntheses. 1-(2-Bromoacetyl)pyrene. To a mixture of $AlCl_3$ (7 g, 51.4 mmol) in CH_2Cl_2 (70 mL), a solution of pyrene (8 g, 39.55 mmol) and 2-bromoacetyl chloride (3.46 mL, 39.55 mmol) in CH_2Cl_2 (100 mL) was added under N_2 atmosphere. The reaction mixture was stirred at room temperature for 3 h. Water (200 mL) was added and phases were separated. Hexane (200 mL) was added to the organic phase, and it was filtrated through silica gel. The organic phase was evaporated to dryness and the precipitate obtained was purified by recrystallization from ethanol (m = 8.9 g, yield = 70%). ^{1}H NMR ($CDCl_3$): 9.3 (1H, d), 8.68−8.28 (8H, m), 4.73 (2H, s).

2-Oxo-2-(pyren-1-yl)ethanesulfonate, Sodium Salt (8). 1-(2-Bromoacetyl)pyrene (1.5 g, 6.46 mmol) and Na_2SO_3 (3.2 g, 25.8 mmol) were dissolved in water−acetone mixture (1:1, 40 mL). The mixture was refluxed for 16 h and evaporated to dryness. Water was added (100 mL) and heated to boiling, after which the solution was filtrated. The solution was allowed to cool, which resulted in crystallization (m = 1.5 g, yield = 67%). ^{1}H NMR (D_2O/DMSO): 8.58 (1H, m), 8.39 (1H, m), 8.20 (1H, m), 8.18 (1H, m), 8.10 (3H, m), 7.98 (2H, m), 4.46 (2H, s).

1-Methyl-3-[2-oxo-2-(pyren-1-yl)ethyl)]-3H-imidazolium Bromide (9). 1-(2-Bromoacetyl)pyrene (280 mg, 0.866 mmol) and *N*-methyl-imidazole (74 mg, 0.91 mmol) were dissolved in a mixture of CH_2Cl_2 (20 mL) and acetonitrile (20 mL). The solution was stirred at room temperature for 4 days, after which the precipitate formed was collected by filtration (m = 330 mg, yield = 94%). ^{1}H NMR (D_2O): 8.68 (1H, m), 8.14−7.39 (12H, m), 3.90 (2H, s).

Purification of HiPco SWNTs. About 150 mg raw HiPco SWNTs (Carbon Nanotechnologies, United States) was accurately weighed and placed in a ceramic crucible. The crucible was inserted into a quartz tube oven, through which humid air was flown. The temperature of the oven was raised at a rate of 5 °C/min to 260 °C and kept there for 1000 min (about 17 h).

Oxidized SWNTs were extracted with aliquots of concentrated HCl until the yellow color of dissolved iron faded. Nitric or sulfuric acid was not used because they oxidize and cut SWNTs.[18] Extracted SWNTs were collected on a polycarbonate membrane (0.2-μm-pore, Millipore) in a stirred-cell system (Spectrum, model S-43-70) and washed with distilled water until the pH of the filtrate was neutral. SWNTs were dried at 70−100 °C in an oven and the procedure (oxidation−extraction−filtration) was repeated to improve the purity. However, during the second cycle, oxidation was conducted at 360 °C for 90 min. The total yield was 71%. The purification process was monitored with X-ray photoelectron spectroscopy (XPS, see Supporting Information).

Modification of Purified SWNTs. Attempts to solubilize SWNTs using compounds **1**, **3**, and **4** failed. The extent of solubilization with compound **2** was minute and without any practical value and it was excluded from further work. In successful modification with compounds **5**−**10**, the general procedure was as follows. The adsorbates **5**−**7** were dissolved in water (at concentration 10−13 mM) and an equivalent amount of NaOH was added to the solutions to deprotonate the sulfonic acid groups. The pH of the solutions was always well above the pK_a of the substituent ammonium group. The adsorbates **8**−**10** were dissolved in pure water (in concentration 0.5−2.5 mM). In adsorption experiments, 1−3 mg purified HiPco SWNTs and 10−15 mL adsorbate solution were added to a glass tube and sonicated in a low-energy ultrasonic bath (Bandelin Sonorex TK52) for 1.0−1.5 h. The SWNT solution was allowed to stand overnight to stabilize and sedimentate the undissolved particles from the black supernatant solution. The supernatant was dialyzed against distilled water (CelluSep T1 or T2 dialysis tubing, Membrane Filtration Products, Inc., MWCO 3500 or 6000−8000, respectively) to remove excess adsorbate molecules from the solution. Water (0.5 L) was changed at least three times with 3-h intervals. For the dialysis of SWNT**9** and SWNT**10**, the dialysis tubing was pretreated with a poly(diallyldimethylammonium)chloride (Aldrich) solution to prevent the adsorption of cationic SWNTs on the tubing walls.

Characterization. The solubility of SWNT**5** (or **9**) was determined with a quartz crystal resonator (QCR). A drop (1 μL) of SWNT**5** or SWNT**9** water solution was allowed to dry on a QCR gold electrode and the respective frequency change was recorded. Mass of dissolved solids was calculated from the Sauerbrey equation[19] and the fraction of dissolved SWNTs (of the total mass) was estimated using the adsorbate surface coverage determined by XPS. The obtained SWNT concentration was used for the calculation of the absorption coefficient as described in the text. UV−vis−NIR spectra were recorded with a Varian Cary 5E spectrophotometer in 10-mm quartz cuvettes. Fluorescence spectra were measured with a Perkin-Elmer LS-5 luminescence spectrophotometer in 10-mm quartz cuvettes. Raman spectra were obtained from solid or solution samples with the excitation wavelengths 1064 and 780 nm. For 1064-nm excitation, we used a Nicolet FT-Raman spectrometer equipped with an Nd:YAG laser and a liquid N_2 cooled Ge detector. For 780-nm excitation, a dispersive Renishaw Ramascope Raman spectrometer was used with a CCD detector. XPS spectra were recorded with a Perkin-Elmer PHI 5400 instrument equipped with a concentric hemispherical electron analyzer. A pass energy of 89.45 eV was used for survey spectra and 35.75 eV for short-range spectra. Monochromatic Al Kα (E = 1486.6 eV) or Mg Kα (E = 1253.6 eV) was used for photoexcitation. The takeoff angle was 45°. The binding energy scale was calibrated with the Au 4f 7/2 peak position (84.00 eV) or (if not possible) with the Si 2p peak position (103.7 eV). To prepare substrates for the XPS measurements, a 100-nm-thick gold layer was evaporated on silanized (1 wt-% 3-aminopropyltriethoxysilane in toluene, 4 min at 60 °C)[20] microscopy slides and a drop of an SWNT solution was dried on the gold surface. The transmission electron microscopy (TEM) images were acquired using an energy-filtered TEM (JEOL 2010) operating at 200 kV. Elemental analysis was carried out with an electron energy loss spectrometer (EELS) coupled to the TEM. An energy filter (Gatan Imaging Filter, GIF) was placed after the fluorescent screen. For sample preparation, a drop of SWNT solution was spread on a copper grid covered by a Formvar and a carbon film. The grids were dried in air. To reduce the carbon contamination, the walls of the sample chamber were cooled at liquid nitrogen temperature. The EELS maps were calculated using a three-window method: the background was fitted using two energy windows before the nitrogen edge; the nitrogen core-loss signal was calculated by subtracting the fitted background from the signal in correspondence to the edge (third energy window).

Results and Discussion

Solubilization of SWNTs in Water. In solubilizing SWNTs in an aqueous solution, only the compounds **5**−**10** were successful (the extent of solubilization with **2** was so small that this compound was excluded from further analysis). Aqueous solutions of SWNT**5**−**10** that have been dialyzed to remove excess adsorbate are usually dark black or gray, except SWNT**7**, which is reddish (see Supporting Information; special care was taken to use mild purification techniques to produce full-length nanotubes for the modification). Freshly prepared solutions are free of any visible particulates, implying the absence of large bundles. This is also supported by transmission electron microscopy (TEM) images, which typically show a mixture of thin bundles and individual nanotubes (see Supporting Information). In addition, mapping nitrogen in the SWNT**5** sample using electron energy loss spectroscopy (EELS) shows that nitrogen is confined to the nanotubes. The stability of dialyzed nanotube solutions varies from months to several days and decreases in the approximate order SWNT**5** > SWNT**9** ≥ SWNT**7**, SWNT**10** > SWNT**6**, SWNT**8**. The SWNT solutions are usually more stable (weeks/months) with excess adsorbate present, which is a manifestation of the reversible nature of the noncovalent modification.[9]

Water-soluble SWNT-PEs were studied with several spectroscopic methods to characterize the interactions between SWNTs and the adsorbate molecules. In the UV−vis−NIR spectra of the modified SWNTs, the most prominent features (Figure 1) are the lowest-energy van Hove transitions S_{11} of the semiconducting SWNTs at 1000−1400 nm. Partially overlapping S_{22} and metallic M_{11} transitions can also be seen at 500−900 nm. Although a total disappearance of the van Hove transitions was recently reported in organic-soluble pyrene-modified SWNTs, the retention of these spectral features has been considered to be characteristic of noncovalent modification in most other studies, contrary to covalent modification.[8g,21] In our case, the presence of these singularity pair transitions after modification indicates that the electronic properties of the nanotubes have not been disturbed. The line widths of the van Hove transitions are related to the size of the SWNT bundles. Individual, isolated tubes have been reported to give rise to sharp, well-resolved peaks.[22] The peaks corresponding to the van Hove transitions in SWNT**5**−**10** are broader, implying some bundling, but comparable to or better resolved than in most of

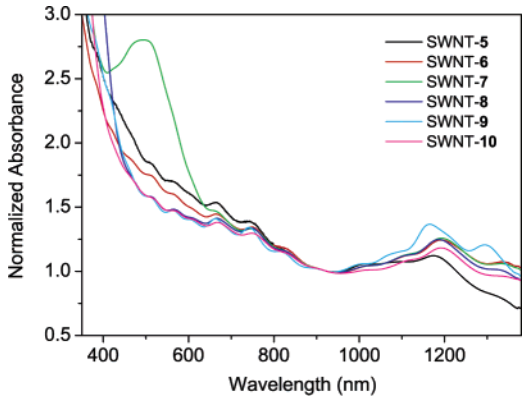

Figure 1. Vis−NIR spectra of modified SWNTs in water. Normalized to 1.00 at 925 nm.

the spectra reported for water-soluble nanotubes, with the exception of peptide-wrapped SWNTs.[3c,8g,23,24] The S_{11} transitions of the modified nanotubes also display a clear pH dependence as reported previously for oxidized nanotubes with surface carboxylate groups and for surfactant-suspended SWNTs.[23,25] In the range 450−800 nm, the spectrum of each pyrene-modified SWNTs follows the same curve, while the naphthalene-modified SWNT**5** and SWNT**6** exhibit a higher absorbance and in the spectrum of SWNT**7** an additional broad and strong peak appears reproducibly at 450−550 nm. The adsorbates **5**−**10** do not absorb in this spectral range and we attribute these features, centered at approximately 500 nm, to the formation of a CT complex between the aminonaphthalene compounds **5**−**7** and SWNTs. Support for this assignment was obtained from other spectroscopic studies (vide infra). Peaks originating from the adsorbates appear in the range 200−400 nm (not shown), but the separation of these features from the sloping SWNT background is prone to large errors, thus hampering their analysis.

The water solubility of the modified SWNTs was calculated from the UV−vis−NIR spectra. The literature data for the absorption coefficient of SWNTs are scarce and inconsistent[26] and, therefore, we have determined it with a quartz crystal microbalance (QCM) resonator using the Sauerbrey equation and the adsorbate surface coverage determined by XPS (vide infra). The coverage-corrected values of the absorption coefficient at 925 nm were $\epsilon = 11.9$ $Lg^{-1}cm^{-1}$ and $\epsilon = 9.4$ $Lg^{-1}cm^{-1}$ for SWNT**5** and SWNT**9**, respectively. In the following, we have used the average value of 10.6 $Lg^{-1}cm^{-1}$ for all derivatized nanotubes. The water solubility of the different modified SWNTs, on the basis of the spectral measurements, was 0.1−0.3 g/L for solutions containing an excess of the adsorbate (Table 1). During dialysis, the SWNT concentration decreased by 15−50% owing to precipitation and dilution. However, we assume that all SWNT solutions remained saturated, since solid SWNTs were present at all preparation stages (during sonication and dialysis), and that these concentrations represent the solubilities of SWNT**5**−**10** with and without excess adsorbate. As seen in Table 1, the solubility of dialyzed pyrene- and naphthalene-modified nanotubes decreases in the order SWNT**5** > SWNT**9** ≥ SWNT**6**, SWNT**7** > SWNT**8** ≥ SWNT**10**, resembling the stability series. The solubility is smaller than that achieved with polymeric solubilizers or dodecylbenzenesulfonate but comparable to that obtained with other surfactants.[5,6,27−29] However, the solutions of dialyzed SWNT**5**−**10** do not contain foreign materials, such as surfactants, and the modified nanotubes are ready for further modification and assembly.[30]

TABLE 1: Water-Solubility and Integral Ratio of the Raman G and D Lines of the Modified and Unmodified HiPco SWNTs

sample	solubility [g/L][a]	I_G/I_D[b]
as-prepared		4.41 (19.8)
purified		4.23 (18.2)
SWNT**5**	0.30 ± 0.07 (0.26 ± 0.04)	2.97 (10.5)
SWNT**6**	0.22 ± 0.02 (0.14 ± 0.02)	3.73 (13.6)
SWNT**7**	0.23 ± 0.02 (0.14 ± 0.02)	3.58 (nd)[c]
SWNT**8**	0.14 ± 0.02 (0.06 ± 0.02)	3.12 (14.2)
SWNT**9**	0.25 ± 0.05 (0.18 ± 0.02)	3.76 (11.5)
SWNT**10**	0.12 ± 0.02 (0.03 ± 0.02)	2.84 (15.4)

[a] Values in parentheses represent solubility after dialysis. Estimated error limits are based on uncertainty in the determination of the absorption coefficient. The values refer to the SWNT material. [b] Excitation wavelength 1064 nm (780 nm in parentheses). [c] Not determined.

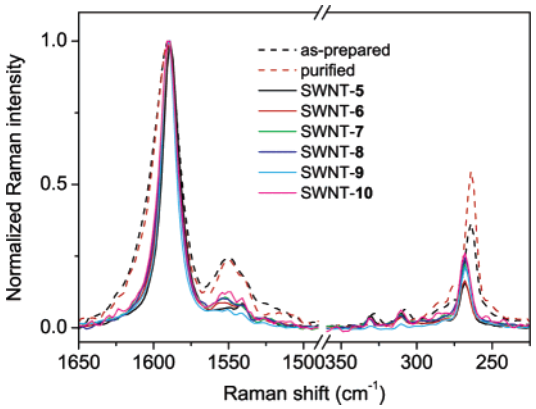

Figure 2. Tangential G mode and radial breathing modes of the modified SWNTs (in an aqueous solution, solid curves) and unmodified SWNTs (powder in capillary, dashed curves). Excitation at 1064 nm. All spectra normalized with respect to the $G^{(+)}$ peak.

Characterization with Raman Spectroscopy. Resonance enhancement of the Raman modes in carbon nanotubes occurs when the excitation energy matches the energy of the interband transitions in SWNTs and, therefore, different tubes are in resonance with different excitation energies. Our Raman analysis was restricted mainly to the semiconducting tubes owing to instrumental limitations. Two excitation wavelengths were used in this work, 1064 and 780 nm, both of which reside in the spectral region of the S_{11} and S_{22} transitions of the semiconducting SWNTs. In case of the higher wavelength, the tubes with diameters in the range of ca. 0.7−0.9 nm are excited, while excitation at 780 nm is in resonance with tubes having diameters of ca. 0.6−0.7 nm or 1.0−1.2 nm.[31]

The Raman spectrum of SWNTs contains three major characteristic regions: the tangential modes (the so-called G bands) at 1540−1600 cm^{-1}, the radial breathing modes (RBM) at 250−350 cm^{-1}, and the disorder-induced D mode at 1270−1300 cm^{-1}. The simultaneous observation of the RBM and G modes confirms that all our aqueous solutions contain SWNTs (Figure 2; for the complete Raman spectra, see Supporting Information). In carbon nanotubes, there are longitudinal and circumferential tangential vibrations, which give rise to the $G^{(+)}$ and $G^{(-)}$ components at 1591 cm^{-1} and 1540−1580 cm^{-1}, respectively. The G band of the modified SWNTs shows a "semiconducting" (narrow) line shape, as expected for the excitation in near-infrared.[31] Upon modification, the line width of the $G^{(+)}$ component becomes narrower and the peak position is downshifted by about 2 cm^{-1} in each case. The intensity of the $G^{(-)}$ component also decreases by 50−75% (Figure 2). This behavior is similar to that reported by Stepanian et al. for solid

samples of pyrene-modified SWNTs and indicates complex formation between the aromatic modifiers and the nanotube side walls.[32] The downshift of the G mode implies *n*-doping of the SWNTs and the extent of the shift is expected to scale with the amount of charge transferred per nanotube carbon atom.[33] For alkalimetal-doped graphite intercalation compounds, downshifts of about 140 cm^{-1}, per electron and per carbon, have been reported.[33] The observed shift of 2 cm^{-1} implies a partial charge transfer of approximately 0.01 electrons per 1 SWNT carbon atom from the adsorbate molecules **5**−**10**. This value has to be considered only a very rough estimate because the changes in the Raman spectra of SWNTs upon *n*-doping are rather complex and without a consistent interpretation. However, similar changes have been reported during the electrochemical reduction of carbon nanotube films.[34]

The radial breathing modes (RBM) involve a radial displacement of the SWNT carbon atoms. The RBM frequency is related to the tube diameter by $\omega_{RBM} = A/d + B$ and, for bundled HiPco tubes, values $A = 239$ $nm^{-1}cm^{-1}$ and $B = 8.5$ cm^{-1} have been used.[35] With 1064-nm excitation, three RBM peaks are resolved corresponding to diameters 0.74, 0.80, and 0.93 nm (in the unmodified samples, two shoulders corresponding to diameters 0.87 nm and 0.89 are also visible, Figure 2). These values are in accordance with the known diameter range of the HiPco tubes (0.7−1.2 nm). Excitation at 780 nm gives only one RBM peak that comes from 0.93-nm tubes. Covalently functionalized SWNT samples usually show a complete loss of radial breathing modes,[36] so their existence is another indicator of noncovalent bonding between the nanotubes and the modifiers. We observe, however, a clear attenuation of the main RBM mode upon modification (Figure 2). The decrease in intensity is probably a consequence of the filling of the conduction band upon *n*-doping (charge transfer), which results in the quenching of the singularity transitions and a concomitant loss of the Raman resonance.[34,37]

The disorder-induced D-mode is caused by vacancies, substitutional heteroatoms, sp^3 defects (covalent modification), finite-size effects, and even bending. The D-mode is observed for all our SWNT samples but its intensity relative to the G-mode does not show any dramatic change upon purification and modification (see Table 1 and Supporting Information). The calculated integral ratio of the G and D lines remains at ca. 4.0−4.5 during purification (1064-nm excitation) and decreases by 10−30% upon modification. This result also indicates noncovalent modification with little damage, since in covalently functionalized SWNTs the D-line intensity is comparable to or even larger than the G-line intensity.[36,38]

Charge Transfer to Nanotubes and the Extent of Modification. Doping of SWNTs has been shown to affect the binding energy (BE) of the nanotube C 1s core electrons in XPS.[39] For pristine SWNTs, the C 1s peak is observed at 284.2−284.6 eV,[40] but charge transfer between SWNTs and adsorbates leads to a shift in the binding energy, upward for *n*-doped and downward for *p*-doped nanotubes.[39] For the purified SWNTs, we observe a BE of 284.3 eV with an asymmetric line shape due to the presence of metallic tubes in the sample, and the peaks are best fitted with a Doniach−Sunjic function convoluted with a Gaussian function.[41] The Gaussian line width is larger for the modified SWNTs than for the unmodified SWNTs (approximately 1.1 eV vs 0.85 eV), which may be caused by the adsorption-induced nonequivalence of the SWNT carbon atoms and the adsorbed molecules (Figure 3). However, a single Gaussian convoluted Doniach−Sunjic component with an asymmetry parameter of 0.21 ± 0.03 can be used to fit all the sample spectra (with the exception of SWNT**9**).

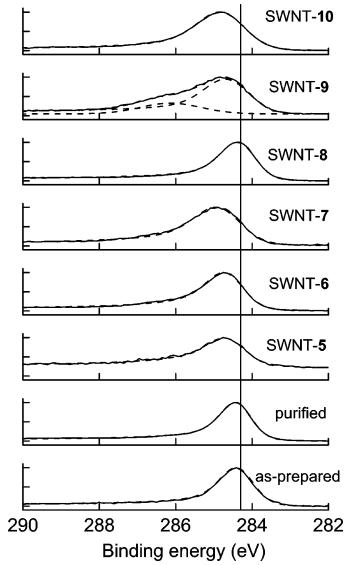

Figure 3. C 1s core level spectra of the modified and unmodified SWNTs. The dashed curves are fits to the Gaussian convoluted Doniach−Sunjic function. The vertical line marks the average BE of the purified SWNTs at 284.3 eV.

The purification procedure results in a negligible (0.04 eV) *n*-doping of the tubes, but a further positive shift of 0.1−0.6 eV in the C 1s binding energy for the modified SWNTs (Table 2) confirms the charge-transfer nature of the interactions, showing that the SWNTs act as electron acceptors and the adsorbates as electron donors. The resolution of the XPS instrument was not high enough to allow the separation of the C 1s peaks due to the adsorbates and nanotube material, which results in average values for the binding energy (work currently in progress utilizes synchrotron-based core electron spectra of the modified nanotubes for a more detailed analysis). In this work, the charge transfer was largest between SWNTs and the pyrene derivative **10**. The SWNTs do not show any substantial amount of oxidized carbon, which has binding energies in the range 286−289 eV.[42] Only for SWNT**9** were two peaks observed, of which the one at 286.1 eV can be assigned to oxidized or sp^3 hybridized carbon atoms. However, the Raman I_G/I_D ratio for SWNT**9** does not indicate any noticeable damage (Table 1), and the origin of this carbon species is not clear at the moment. Pristine SWNTs do not contain nitrogen or sulfur, but the modified SWNTs contain small amounts of N, S, or both, in addition to C and O, which is due to chemisorbed oxygen, substrate oxides, and the adsorbate molecules (Table 2).

In the noncovalent modification of SWNTs, an important parameter is the extent of adsorption. In case of ionic, aromatic modifiers, the relevant measures of adsorption are the surface coverage and the surface charge density. The former refers to the portion of the nanotube surface covered by the aromatic part of the adsorbate (assuming coplanar geometry), while the latter is the density of adsorbed ionic charges on the surface. The determination of the adsorbate concentration using the absorbance spectra of the modified SWNTs is very difficult because of the large varying background due to the nanotubes. In this work, the elemental composition of the modified SWNTs was determined by XPS. Several measurements were done from each sample to account for local variations. The average surface coverage, calculated from the nitrogen or sulfur atomic concentrations, was 10−60%, depending on the adsorbate. In the

TABLE 2: Ratios of Atomic Concentrations,[a] Surface Coverage[b] θ, Ionic Charge Density[c] ρ, and C 1s Core Level Shift[d] ΔE_C of the Modified and Unmodified SWNTs

sample	[*C*]/[*N*]	[*C*]/[*S*]	$\theta(N)$ [%]	$\theta(S)$ [%]	$\rho(N)$	$\rho(S)$	ΔE_C [eV]
as-prepared							-0.04 ± 0.07
purified							0.00 ± 0.09
SWNT**5**	30 ± 6	36 ± 3	21 ± 5	15 ± 2	0.10 ± 0.02	0.08 ± 0.01	0.21 ± 0.08
SWNT**6**	60 ± 20	31 ± 4	9 ± 5	19 ± 4	0.05 ± 0.02	0.10 ± 0.02	0.24 ± 0.10
SWNT**7**	28 ± 12	18 ± 4	29 ± 15	59 ± 32	0.15 ± 0.07	0.30 ± 0.16	0.41 ± 0.11
SWNT**8**		44 ± 5		31 ± 6		0.08 ± 0.01	0.14 ± 0.06
SWNT**9**	25 ± 5		31 ± 10		0.08 ± 0.03		0.24 ± 0.37
SWNT**10**	36		42		0.10		0.61

[a] Average from several scans at different sample locations. Standard deviation of the results is shown in every column. [b] Expressed as the percentage of the nanotube surface covered by the aromatic part of the adsorbate assuming coplanar adsorption. The *N* and *S* atomic concentrations in the XPS spectra were used to calculate $\theta(N)$ and $\theta(S)$, respectively. [c] In units of ionic charges per one aromatic ring (hexagon) on SWNT surface. Calculated from the *N* or *S* atomic concentrations. [d] The shift is calculated relative to the purified sample.

calculation, we have assumed the aromatic plane of the adsorbate molecule to lie flat on the nanotube surface.[32] The surface coverage was high, 30−40%, for the pyrene derivatives **8**−**10**, while the substituted naphthalenes **5** and **6** exhibited considerably smaller values. Interestingly, 5-aminonaphthalene-2-sulfonate (**7**) exhibited an anomalously large surface coverage. All the values in Table 2 are larger than those reported for anthracene derivatives, which were, however, determined by a different technique.[9]

On the other hand, a more informative parameter is the surface charge density due to adsorbed ionic groups. This parameter displays considerably less deviation from sample to sample, being in the range 0.08−0.10 charges per SWNT hexagon for most samples, independent of the size of either the aromatic part or the side chain. This implies that the limiting factor in the adsorption is the electrostatic repulsion of like charges on the SWNT side walls, which, in general, results in a smaller surface coverage for naphthalenes than for the bulkier pyrenes. Interestingly, SWNT**7** is the only one exhibiting a substantially larger value. The average surface charge per nanotube ring can be unambiguously calculated from the experimental data, but if we want to estimate the *linear* ionic charge density of the modified SWNTs, we can model the nanotube mixture with (12, 0) zigzag or (7, 7) armchair tubes, both having a diameter of ca. 0.95 nm (consistent with the Raman data). The length of the 1D unit cell along the axis of a (n, m) tube is given by $T = \sqrt{3}\, a(n^2 + nm + m^2)^{1/2}/d_R$ and the number of carbon rings in the unit cell by $N = 2(n^2 + nm + m^2)/d_R$, where a is the length of the graphene sheet unit vector (0.246 nm) and d_R is the highest common divisor of $2n + m$ and $2m + n$.[43] For modified nanotubes SWNT**5**, **6**, **8**−**10**, this leads to an average value of ca. 4−5 charges/nm. Comparison with common polycations and polyanions, for example, poly(diallyldimethylammonium) and poly(styrene sulfonate) (PDADMA and PSS, linear charge densities ca. 1.6 and 6.25 charges/nm, respectively),[44] shows that the modified nanotubes can be regarded as highly charged polyelectrolytes.

Effect of the Adsorbate Structure. The exact nature of the adsorbate−nanotube interaction and its dependence on the adsorbate structure are core issues for the noncovalent modification of SWNTs. Generally, $\pi-\pi$ stacking interactions and a coplanar orientation are assumed for aromatic adsorbates.[8a−c,e,f,9,32] With compounds **5**−**10**, our XPS (and Raman) results all show charge transfer from the adsorbates to the nanotubes, indicating a close contact between the donor (aromatic compound) and the acceptor (nanotube). However, there is no clear correlation between the amount of charge transfer (shift in the C 1s binding energy) and solubility, stability, or surface charge density. This implies that although CT interactions exist in all studied systems, their role is not decisive. The $\pi-\pi$ interactions depend on the size and shape of the aromatic system and its substitution while the charge-transfer interactions rely on the donor−acceptor properties of the components (also affected by the substituents). In the $\pi-\pi$ stacking, the hydrophobic effects are more important with the bulky pyrenes than with naphthalenes. Steric factors, which set constraints to the geometry of the SWNT−adsorbate adduct, influence both modes of interaction. Unfortunately, no uniform set of electrochemical data or ionization potentials for the compounds **1**−**10** is available. Although substituted benzenes display charge-transfer interactions with carbon nanotubes, the failure of the compound **1** to dissolve SWNTs is understandable considering the small size of the aromatic system and the steric hindrance caused by the sulfonate groups. In the naphthalene sulfonate series **2**−**7**, all the successful solubilizing agents contain a free amino group in the ring adjacent to that of the sulfonate group, which suggests an interplay of electronic and steric factors. The aromatic core of naphthalene is rather small and even anthracene derivatives (with no amino substitution) displayed a relatively low affinity toward the nanotubes.[9] On the other hand, the large pyrene system strongly adsorbs on the SWNT side wall. Theoretical calculations imply an interaction energy of ca. 30 kJ/mol for nanotubes of similar diameter as in this work, and the optimal geometry of an adsorbed pyrene molecule on the nanotube surface is a so-called 1/2-staggered conformation, where the pyrene rings have been shifted by one-half of the length of the ring with respect to the surface rings.[32]

Some further insight in the mode of adsorption is provided by the fluorescence spectra of the modified nanotubes (Figure 4). All solutions of the dialyzed and modified nanotubes exhibit the fluorescence spectra of the adsorbates, which is a further indication of adduct formation. However, the adsorbate fluorescence is generally markedly quenched. This is in contradiction with the work of Murray et al., who did not observe any quenching of the anthracene fluorescence in their nanotube samples.[9] On the other hand, the pyrene fluorescence is strongly quenched in nanotubes functionalized with tethered pyrenes owing to energy transfer to the nanotube.[45] For the pyrene-modified nanotubes SWNT**8**−**10**, the fluorescence spectra are very similar in shape to those of the adsorbate solutions (of similar nominal concentration) with the exception of two factors. First, the fluorescence spectra are red-shifted by approximately 5 nm, which indicates electronic communication between the (excited) adsorbates and nanotubes and is in accordance with the results reported for anthracene-modified SWNTs.[9] Second, the excimer fluorescence (above 450 nm) is much less pronounced in the nanotube samples, although the nominal adsorbate concentration is higher than in the adsorbate solutions. For nanotubes with tethered pyrenes, excimer fluorescence is present, and this result indicates that the pyrene derivatives **8**−**10**

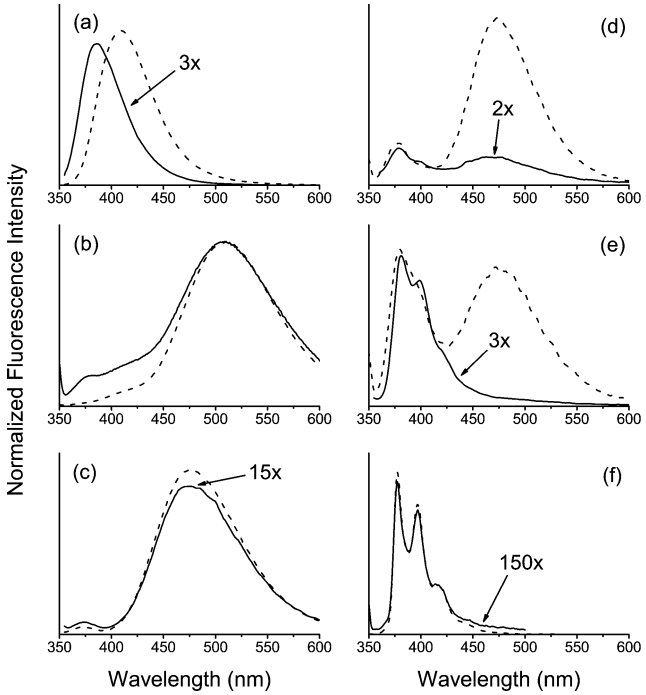

Figure 4. Fluorescence emission ($\lambda_{ex} = 340$ nm) spectra of (a) SWNT**5** (pH 5.3, 23.0 μM, solid line) and **5** (pH 4.8, 9.8 μM, dashed line), (b) SWNT**6** and **6** (10 μM), (c) SWNT**7** (8.2 μM) and **7** (1.0 μM), (d) SWNT**8** (3.7 μM) and **8** (1.0 μM), (e) SWNT**9** (15.0 μM) and **9** (1.0 μM), and (f) SWNT**10** (4.1 μM) and **10** (1.0 μM) in water. Intensities have been divided by the (nominal) concentration of adsorbate present in solution (in parentheses).

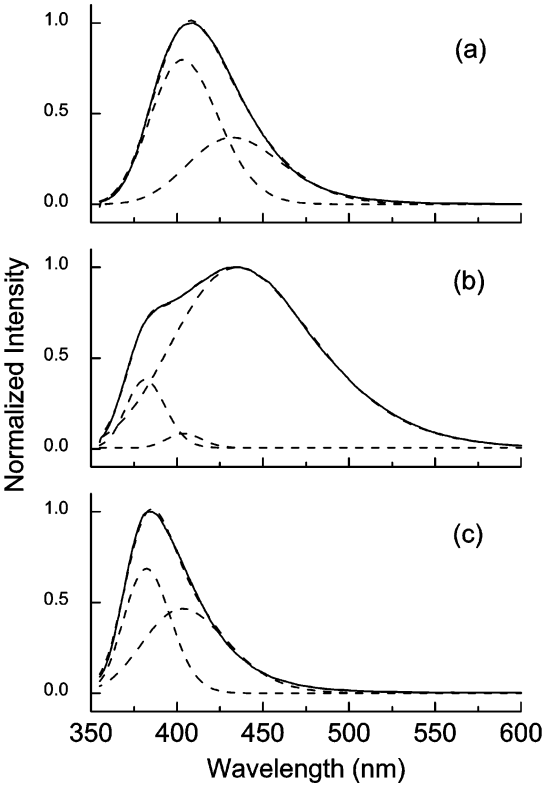

Figure 5. Fluorescence emission spectra (solid curves, $\lambda_{ex} = 340$ nm) and their deconvolution to Gaussian peaks (dashed curves; the sum curve also shown) for (a) **5** at pH 6.3 (deconvoluted peaks at 403 nm, 432 nm), (b) **5** at pH 13.4 (382 nm, 403 nm, 432 nm), and (c) SWNT**5** at pH 6.1 (382 nm, 403 nm).

are adsorbed on the nanotube surface as monomers in a coplanar fashion. SWNT**8** makes an exception by displaying strong excimer fluorescence, although less than **8** in aqueous solution. Three possible explanations can be given for the excimer formation in this case. The excimer fluorescence may originate from regions where two nanotubes cross each other or from pyrene molecules adsorbed in a dimeric form. However, these explanations are unlikely because excimer fluorescence is not observed for the other pyrene-modified SWNTs. Therefore, the adsorbate **8** probably desorbs relatively easily from the surface, thus giving rise to dimer fluorescence at higher wavelengths. This implies a low solubility and stability for SWNT**8** in aqueous solutions, which is in accordance with other observations.

For naphthalenes, it is plausible to assume that charge-transfer effects involving the amino group may play an important role in the interaction between the small naphthalene sulfonates and carbon nanotubes. The fluorescence spectra of the naphthalene-derivatized nanotubes are interesting and clarify the role of the amino group. While the spectra of SWNT**6** and SWNT**7** are identical (although quenched) to that of **6** and **7**, SWNT**5** displays a hypsochromic shift of the fluorescence maximum from 410 nm (**5** in a neutral solution) to 385 nm (Figure 4). To understand this shift, we have studied the fluorescence of **5** as a function of pH, which is complicated because of the presence of three ionizable groups (see Supporting Information). The fluorescence of SWNT**5** at pH $\geq$ 6 can be deconvoluted to two contributions at ca. 380 and 405 nm (Figure 5). In solutions of **5**, the peak at 410 nm dominates the spectrum in the range $4 \leq$ pH ≤ 10, above which the peak shifts to ca. 430 nm with a shoulder developing at ca. 385 nm in very basic solutions. On the basis of the ground-state and excited-state pK_a values (pK_a(NH_3^+) = 3.4, pK_a^*(NH_3^+) = 1.4, and pK_a(OH) = 10.0 for 7-amino-1-hydroxynaphthalene, and pK_a^*(NH_2) = 12.3 for 2-aminonaphthalene, where the superscript * stands for the excited-state pK_a value),[46] we attribute the (deconvoluted) 403-nm fluorescence to the species with neutral amino and hydroxyl groups (**5**$^-$) and the shoulder at 385 nm to the excited **5**$^{3-}$ anion with deprotonated O^- and NH^- groups (the 432-nm band most probably originates from a dianion with neutral amino moiety). The observation of the 385-nm fluorescence in SWNT**5** solutions already at a neutral pH indicates greatly facilitated deprotonation of the excited amino group on the nanotube surface. This implies strong interactions between the nanotube and the amino nitrogen of **5**, which enables the delocalization of nitrogen electrons to the nanotube. Although there are amino groups in all the naphthalene derivatives **4**−**7**, the fluorescence spectra of **6** and **7** display practically no pH dependence, and the similarity of the nanotube and the adsorbate spectra does not exclude the possibility of an amino-mediated interaction also in these cases. In fact, the high surface charge density, the intense charge-transfer band in the visible spectrum, and the large positive shift in the C 1s binding energy all suggest that **7** interacts with the nanotubes via the amino group. The specific role of the hydroxy substituent in **5** is not certain at the moment. The naphthalene sulfonates **2** and **3**, which could not solubilize the SWNTs, do not have a free amino group. If the amino groups are involved in the charge-transfer interaction with the nanotubes, the strength of the interaction is supposed to increase with the basicity of the NH_2 group (during adsorption, the amino group was not protonated because of the high pH of the solutions). The pK_a values of the ammonium group in compounds **5**−**7** are ca. 3.7−3.8, but in **4** the amino nitrogen is a weaker base (pK_a = 2.8).[46a,47] Although the difference in basicity is small, it correlates with the solubilizing properties of the compounds. However, in **3** the nitrogen atom is even more basic

($pK_a = 4.5$)[48] and the compound is a better donor than **5**−**7**. In the compound **3**, the steric interactions between the bulky methyl groups and the hydrogen at the position 4 of naphthalene hamper the approach of nitrogen close to the nanotube surface.

The results presented above, therefore, suggest that for small aromatic adsorbates, like naphthalenes and probably also anthracenes, the $\pi-\pi$ stacking effects are less important than charge-transfer interactions involving basic (or acidic) substituents. However, the substituents play a dual role because bulky groups can sterically prevent close contacts with the nanotube surface. With naphthalene sulfonates **5**−**7**, charge transfer involving amino substituents stabilizes the SWNT−adsorbate adduct. Also for the pyrene-modified nanotubes, the highest stability was found in the case of the adsorbates **9** and **10**, both of which contain an ionic group that can be involved in cation$-\pi$ interactions with carbon nanotubes.[16,49] With the charged ammonium substituent, these interactions can be substantial and lead to physical cross-linking of the modified nanotubes, thus explaining the low solubility of SWNT**10**.

Conclusions

We have prepared anionic and cationic water-soluble full-length SWNT polyelectrolytes via noncovalent modification of the nanotubes using ionic pyrene and naphthalene derivatives. The modified nanotubes were characterized in solution by UV−vis−NIR, fluorescence, and Raman spectroscopy and in the solid state by XPS. UV−vis−NIR and Raman spectroscopy confirm that the modification does not alter the electronic structure of the SWNTs and that the interactions between the tubes and the adsorbates are mainly noncovalent in nature. Charge transfer from the adsorbates to the nanotubes is indicated by the positive shifts in the C 1s binding energy. Adsorbates containing an amino group show an enhanced interaction with the nanotubes. Specific interactions between the substituents and the nanotube surface (charge transfer, cation$-\pi$ interactions) are important, especially with small aromatic molecules such as naphthalenes. The ionic surface charge density of the modified nanotubes is almost constant, probably limited by electrostatic repulsion between the ionic adsorbates, and the modified SWNTs can be regarded as highly charged polyelectrolytes owing to the high linear ionic charge density. The stability and solubility of all the SWNT polyanions and polycations studied is high enough to enable their processing in an aqueous environment and introduction into self-assembled multilayer structures.

Acknowledgment. Financial support from the Academy of Finland (Grant No. 106215) and from the Graduate School of Materials Research (H.P.) is gratefully acknowledged. The authors thank Dr. Carita Kvarnström and Ms. Virpi Väänänen for assistance in Raman measurements, Mr. Jussi-Matti Kauko for the QCM measurements, and Prof. Jouko Kankare for helpful discussions.

Supporting Information Available: Fe 2p core level spectra during purification, vis−NIR spectra of unmodified SWNTs, a photograph of the aqueous solutions, TEM image, EELS nitrogen map of SWNT**5**, XPS survey scans, pH-dependence of the fluorescence emission spectra of the compounds **5**−**7** and SWNT**5**, and complete Raman spectra of all SWNT samples. This material is available free of charge via the Internet at http://pubs.acs.org.

References and Notes

(1) (a) Reich, S.; Thomsen, C.; Maultzsch, J. *Carbon Nanotubes. Basic Concepts and Physical Properties*; Wiley-VCH: Weinheim, Germany, 2004. (b) Terrones, M. *Annu. Rev. Mater. Res.* **2003**, *33*, 419. (c) Avouris, P. *Acc. Chem. Res.* **2002**, *35*, 1026. (d) Dai, H. *Acc. Chem. Res.* **2002**, *35*, 1035. (e) Ouyang, M.; Huang, J.-L.; Lieber, C. M. *Acc. Chem. Res.* **2002**, *35*, 1018.

(2) (a) Niyogi, S.; Hamon, M. A.; Hu, H.; Zhao, B.; Bhowmik, P.; Sen, R.; Itkis, M. E.; Haddon, R. C. *Acc. Chem. Res.* **2002**, *35*, 1105. (b) Sun, Y.-P.; Fu, K.; Lin, Y.; Huang, W. *Acc. Chem. Res.* **2002**, *35*, 1096. (c) Hirsch, A. *Angew. Chem., Int. Ed.* **2002**, *41*, 1853. (d) Tasis, D.; Tagmatarchis, N.; Georgakilas, V.; Prato, M. *Chem. Eur. J.* **2003**, *9*, 4000. (e) Dyke, C. A.; Tour, J. M. *Chem. Eur. J.* **2004**, *10*, 812.

(3) (a) Zhao, B.; Hu, H.; Haddon, R. C. *Adv. Funct. Mater.* **2004**, *14*, 71. (b) Zhang, L.; Kiny, V. U.; Peng, H.; Zhu, J.; Lobo, R. F. M.; Margrave, J. L.; Khabashesku, V. N. *Chem. Mater.* **2004**, *16*, 2055. (c) Pompeo, F.; Resasco, D. E. *Nano Lett.* **2002**, *2*, 369. (d) Shiral Fernando, K. A.; Lin, Y.; Sun, Y.-P. *Langmuir* **2004**, *20*, 4777.

(4) Jiang, L.; Gao, L.; Sun, J. *J. Colloid Interface Sci.* **2003**, *260*, 89.

(5) Islam, M. F.; Rojas, E.; Bergey, D. M.; Johnson, A. T.; Yodh, A. G. *Nano Lett.* **2003**, *3*, 269.

(6) O'Connell, M. J.; Boul, P.; Ericson, L. M.; Huffman, C.; Wang, Y.; Haroz, E.; Kuper, C.; Tour, J.; Ausman, K. D.; Smalley, R. E. *Chem. Phys. Lett.* **2001**, *342*, 265.

(7) (a) Li, H.; Zhou, B.; Lin, Y.; Gu, L.; Kang, W.; Shiral Fernando, K. A.; Kumar, S.; Allard, L. F.; Sun, Y.-P. *J. Am. Chem. Soc.* **2004**, *126*, 1014. (b) Guldi, D. M.; Rahman, G. M. A.; Jux, N.; Tagmatarchis, N.; Prato, M. *Angew. Chem., Int. Ed.* **2004**, *43*, 5526.

(8) (a) Chen, R. J.; Zhang, Y.; Wang, D.; Dai, H. *J. Am. Chem. Soc.* **2001**, *123*, 3838. (b) Nakashima, N.; Tomonari, Y.; Murakami, H. *Chem. Lett.* **2002**, *31*, 638. (c) Xin, H.; Woolley, A. T. *J. Am. Chem. Soc.* **2003**, *125*, 8710. (d) Gómez, F. J.; Chen, R. J.; Wang, D.; Waymouth, R. M.; Dai, H. *J. Chem. Soc., Chem. Commun.* **2003**, 190. (e) Petrov, P.; Stassin, F.; Pagnoulle, C.; Jérôme, R. *J. Chem. Soc., Chem. Commun.* **2003**, 2904. (f) Liu, L.; Wang, T.; Li, J.; Guo, Z.-X.; Dai, L.; Zhang, D.; Zhu, D. *Chem. Phys. Lett.* **2003**, *367*, 747. (g) Shiral Fernando, K. A.; Lin, Y.; Wang, W.; Kumar, S.; Zhou, B.; Xie, S.-Y.; Cureton, L. T.; Sun, Y.-P. *J. Am. Chem. Soc.* **2004**, *126*, 10234.

(9) Zhang, J.; Lee, J.-K.; Wu, Y.; Murray, R. W. *Nano Lett.* **2003**, *3*, 403.

(10) Brown, A. P.; Anson, F. C. *J. Electroanal. Chem.* **1977**, *83*, 203.

(11) Hunter, C. A. *Chem. Soc. Rev.* **1994**, *23*, 101.

(12) Star, A.; Han, T.-R.; Gabriel, J.-C. P.; Bradley, K.; Grüner, G. *Nano Lett.* **2003**, *3*, 1421.

(13) Shim, M.; Javey, A.; Wong Shi Kam, N.; Dai, H. *J. Am. Chem. Soc.* **2001**, *123*, 11512.

(14) Kong, J.; Dai, H. *J. Phys. Chem. B* **2001**, *105*, 2890.

(15) Bradley, K.; Gabriel, J.-C. P.; Briman, M.; Star, A.; Grüner, G. *Phys. Rev. Lett.* **2003**, *91*, 218301.

(16) Bradley, K.; Briman, M.; Star, A.; Grüner, G. *Nano Lett.* **2004**, *4*, 253.

(17) (a) Sun, Y.; Wilson, S. R.; Schuster, D. I. *J. Am. Chem. Soc.* **2001**, *123*, 5348. (b) Perepichka, D. F.; Wudl, F.; Wilson, S. R.; Sun, Y.; Schuster, D. I. *J. Mater. Chem.* **2004**, *14*, 2749.

(18) Liu, J.; Rinzler, A. G.; Dai, H.; Hafner, J. H.; Bradley, R. K.; Boul, P. J.; Lu, A.; Iverson, T.; Shelimov, K.; Huffman, C. B.; Rodriguez-Macias, F.; Shon, Y.-S.; Lee, T. R.; Colbert, D. T.; Smalley, R. E. *Science* **1998**, *280*, 1253.

(19) Sauerbrey, G. *Z. Phys.* **1959**, *155*, 206.

(20) Petri, D. F. S.; Wenz, G.; Schunk, P.; Schimmel, T. *Langmuir* **1999**, *15*, 4520.

(21) Dyke, C. A.; Tour, J. M. *Chem. Eur. J.* **2004**, *10*, 812.

(22) O'Connell, M. J.; Bachilo, S. M.; Huffman, C. B.; Moore, V. C.; Strano, M. S.; Haroz, E. H.; Rialon, K. L.; Boul, P. J.; Noon, W. H.; Kittrell, C.; Ma, J.; Hauge, R. H.; Weisman, R. B.; Smalley, R. E. *Science* **2002**, *297*, 593.

(23) Zhao, W.; Song, C.; Pehrsson, P. E. *J. Am. Chem. Soc.* **2002**, *124*, 12418.

(24) Zorbas, V.; Ortiz-Acevedo, A.; Dalton, A. B.; Yoshida, M. M.; Dieckmann, G. R.; Draper, R. K.; Baughman, R. H.; Jose-Yacaman, M.; Musselman, I. H. *J. Am. Chem. Soc.* **2004**, *126*, 7222.

(25) Strano, M. S.; Huffman, C. B.; Moore, V. C.; O'Connell, M. J.; Haroz, E. H.; Hubbard, J.; Miller, M.; Rialon, K.; Kittrell, C.; Ramesh, S.; Hauge, R. H.; Smalley, R. E. *J. Phys. Chem. B* **2003**, *107*, 6979.

(26) (a) Zhou, B.; Lin, Y.; Li, H.; Huang, W.; Connell, J. W.; Allard, L. F.; Sun, Y.-P. *J. Phys. Chem. B* **2003**, *107*, 13588. (b) Zhao, B.; Itkis, M. E.; Niyogi, S.; Hu, H.; Zhang, J.; Haddon, R. C. *J. Phys. Chem. B* **2004**, *108*, 8136. (c) Landi, B. J.; Ruf, H. J.; Worman, J. J.; Raffaelle, R. P. *J. Phys. Chem. B* **2004**, *108*, 17089.

(27) Ikeda, A.; Hayashi, K.; Konishi, T.; Kikuchi, J. *J. Chem. Soc., Chem. Commun.* **2004**, 1334.

(28) Star, A.; Steuerman, D. W.; Heath, J. R.; Stoddart, J. F. *Angew. Chem., Int. Ed.* **2002**, *41*, 2508.

(29) Zheng, M.; Jagota, A.; Semke, E. D.; Diner, B. A.; McLean, R. S.; Lustig, S. R.; Richardson, R. E.; Tassi, N. G. *Nat. Mater.* **2003**, *2*, 338.

(30) Some batches of HiPco SWNTs may show unusually high solubility in pure water owing to a high concentration of defects (see ref 17b), which makes the direct comparison between the data from different authors difficult. The batch used in our work did not exhibit any water solubility even after several hours of sonication.

(31) Weisman, R. B.; Bachilo, S. M. *Nano Lett.* **2003**, *3*, 1235.

(32) Stepanian, S. G.; Karachevtsev, V. A.; Glamazda, A. Y.; Dettlaff-Weglikowska, U.; Adamowicz, L. *Mol. Phys.* **2003**, *101*, 2609.

(33) Rao, A. M.; Eklund, P. C.; Bandow, S.; Thess, A.; Smalley, R. E. *Nature* **1997**, *388*, 257.

(34) (a) Kavan, L.; Rapta, P.; Dunsch, L. *Chem. Phys. Lett.* **2000**, *328*, 363. (b) Kavan, L.; Dunsch, L. *ChemPhysChem* **2003**, *4*, 944.

(35) Kukovecz, A.; Kramberger, C.; Georgakilas, V.; Prato, M.; Kuzmany, H. *Eur. Phys. J. B* **2002**, *28*, 223.

(36) Bahr, J. L.; Yang, J.; Kosynkin, D. V.; Bronikowski, M. J.; Smalley, R. E.; Tour, J. M. *J. Am. Chem. Soc.* **2001**, *123*, 6536.

(37) (a) Kazaoui, S.; Minami, N.; Jacquemin, R.; Kataura, H.; Achiba, Y. *Phys. Rev. B* **1999**, *60*, 13339. (b) Kukovecz, A.; Pichler, T.; Pfeiffer, R.; Kramberger, C.; Kuzmany, H. *Phys. Chem. Chem. Phys.* **2003**, *5*, 582.

(38) Balasubramanian, K.; Friedrich, M.; Jiang, C.; Fan, Y.; Mews, A.; Burghard, M.; Kern, K. *Adv. Mater.* **2003**, *15*, 1515.

(39) Graupner, R.; Abraham, J.; Vencelová, A.; Seyller, T.; Hennrich, F.; Kappes, M. M.; Hirsch, A.; Ley, L. *Phys. Chem. Chem. Phys.* **2003**, *5*, 5472.

(40) (a) Larciprete, R.; Lizzit, S.; Botti, S.; Cepek, C.; Goldoni, A. *Phys. Rev. B* **2002**, *66*, 121402. (b) Baker, S. E.; Cai, W.; Lasseter, T. L.; Weidkamp, K. P.; Hamers, R. J. *Nano Lett.* **2002**, *2*, 1413. (c) Banerjee, S.; Wong, S. S. *J. Phys. Chem. B* **2002**, *106*, 12144.

(41) (a) Suzuki, S.; Bower, C.; Kiyokura, T.; Nath, K. G.; Watanabe, Y.; Zhou, O. *J. Electron. Spectrosc. Relat. Phenom.* **2001**, *114*−*116*, 225. (b) Goldoni, A.; Larciprete, R.; Gregoratti, L.; Kaulich, B.; Kiskinova, M.; Zhang, Y.; Dai, H.; Sangaletti, L.; Parmigiani, F. *Appl. Phys. Lett.* **2002**, *80*, 2165.

(42) Kovtyukhova, N. I.; Mallouk, T. E.; Pan, L.; Dickey, E. C. *J. Am. Chem. Soc.* **2003**, *125*, 9761.

(43) Dresselhaus, M. S.; Dresselhaus, G.; Saito, R. *Carbon* **1995**, *33*, 883.

(44) (a) Mattison, K. W.; Dubin, P. L.; Brittain, I. J. *J. Phys. Chem. B* **1998**, *102*, 3830. (b) van der Maarel, J. R. C.; Groot, L. C. A.; Hollander, J. G.; Jesse, W.; Kuil, M. E.; Leyte, J. C.; Leyte-Zuiderweg, L. H.; Mandel, M.; Cotton, J. P.; Jannink, G.; Lapp, A.; Farago, B. *Macromolecules* **1993**, *26*, 7295.

(45) (a) Qu, L.; Martin, R. B.; Huang, W.; Fu, K.; Zweifel, D.; Lin, Y.; Sun, Y.-P.; Bunker, C. E.; Harruff, B. A.; Gord, J. R.; Allard, L. F. *J. Chem. Phys.* **2002**, *117*, 8089. (b) Martin, R. B.; Qu, L.; Lin, Y.; Harruff, B. A.; Bunker, C. E.; Gord, J. R.; Allard, L. F.; Sun, Y.-P. *J. Phys. Chem. B* **2004**, *108*, 11447. (c) Álvaro, M.; Atienzar, P.; Bourdelande, J. L.; García, H. *Chem. Phys. Lett.* **2004**, *384*, 119.

(46) (a) Ellis, D. W.; Rogers, L. B. *Spectrochim. Acta* **1964**, *20*, 1709. (b) Rosebrook, D. D.; Brandt, W. W. *J. Phys. Chem.* **1966**, *70*, 3857.

(47) Bryson, A. *Trans. Faraday Soc.* **1951**, *47*, 522.

(48) Chen, W.; Tomalia, D. A.; Thomas, J. L. *Macromolecules* **2000**, *33*, 9169.

(49) Fukushima, T.; Kosaka, A.; Ishimura, Y.; Yamamoto, T.; Takigawa, T.; Ishii, N.; Aida, T. *Science* **2003**, *300*, 2072.